

Three-dimensional structure of Al^{3+} -containing peptides by NMR and molecular modeling study: complexation of a thymic hormone

J.-P. Laussac ^{a,*}, P. Orlewski ^b, M.-T. Cung ^b

^a *Laboratoire de Chimie de Coordination du CNRS, 205, route de Narbonne, 31077 Toulouse Cedex, France*

^b *Laboratoire de Chimie Physique Macromoléculaire, CNRS URA 494, ENSIC-INPL, 1, rue Grandville, BP 451, 54001 Nancy Cedex, France*

Received 23 January 1995; in revised form 14 April 1995

Contents

Abstract	179
1. Introduction	180
2. Experimental	181
2.1. ^1H NMR experiments	181
2.2. Molecular modeling	181
3. Results and discussion	182
3.1. Choice of solvent	182
3.2. One dimensional ^1H NMR studies	183
3.3. Two-dimensional ^1H NMR studies	184
3.4. Secondary structure	186
3.5. Tertiary structure	187
4. Conclusion	189
Acknowledgements	189
References	190

Abstract

The biological coordination chemistry of aluminum has received only limited attention until the last decade. To this end, the interaction between aluminum and thymulin, a linear nonapeptide of thymic origin isolated from serum, was investigated by using high resolution NMR spectroscopy. These experiments were performed in two different solvents, namely DMSO-d_6 and the so-called cryoprotective mixture (water + DMSO), i.e. a mixture that resembles water in many properties. NMR data analysis indicates the existence of one type of complex with a 1:2 stoichiometry, associating two peptide molecules and one Al^{3+} cation.

* Corresponding author.

In this complex the Asn⁹ carboxylate C-terminal group and the Ser⁴ hydroxyl group are ligated to the metal. The three-dimensional structure of the 1:2 Al³⁺–thymulin complex was determined by distance geometry calculations and restrained molecular dynamics simulations. Distance geometry calculations were performed with the Biosym DG II program using the NOE interproton distances as constraints. Further structural analysis was carried out by restrained molecular dynamics calculations with the Biosym DISCOVER program.

Keywords: Aluminium; Thymulin; NMR spectroscopy; Three-dimensional structures

1. Introduction

Although aluminum is one of the most common elements in the earth's crust and in sea water, strong interest has only recently arisen because of its biological roles [1–5]. This breakthrough has been stimulated by the discovery that increased amounts of this metal occur in several human brain diseases. Indeed, elevated concentrations of aluminum have been observed in the brains of patients suffering from dialysis dementia, a progressive and usually fatal neurological syndrome encountered in chronic hemodialysis [6,7] and in senile and presenile dementia of the Alzheimer type [8,9], and have been implicated in the etiology of these diseases. However, the biochemical processes and the molecular mechanisms by which aluminum may exert its neurotoxicity remain poorly understood and controversial [10].

A plausible mechanism of action may lie in the direction of aluminum interference with some essential reactions. For example, hexokinase, a magnesium-dependent enzyme responsible for glucose phosphorylation, is inhibited by aluminum [11] as well as other enzyme systems directly related to neuronal functions [12]. Consequently, studies on the interaction of ATP with Al³⁺ have appeared in the recent literature showing that Al³⁺ binds strongly basic phosphate groups [13–16]. Similarly, Al³⁺ interacts with a large number of biomolecules [4]. Its association both with purified DNA [17,18] and with the acid protein–DNA complex of the nuclear chromatin has been demonstrated [19]. Transferrin interacts with two Al³⁺ and is the main protein carrier of Al³⁺ in plasma [20]. Bovine brain calmodulin has been found to bind three Al³⁺ cations per mole of protein [21]. Recently, a study of Al³⁺ binding to peptides representing the C-terminal phosphorylation domain of the neurofilament protein midsize subunit has been reported [22].

Curiously, only a few reports concern the knowledge of the secondary and tertiary structure of these biomolecular Al³⁺ complexes in solution [23–25]. In fact the particular chemistry of aluminum (see Ref. [5]) can be addressed. Except for the phosphate groups which are the strongest Al³⁺ binders, in proteins and in peptides the most likely Al³⁺-binding sites are the oxygen atoms. Proteins and peptides do not strongly bind Al³⁺, barely competing with Al³⁺ hydrolysis. Furthermore, the reactions of Al³⁺ are complicated by the existence of Al³⁺ as different species in aqueous solution depending on ionic strength, pH, temperature, etc. Thus the choice of an adequate solvent to obtain spectroscopic structural information on these systems seems to be a crucial step (vide infra).

In that context, it is of prime importance to have a better knowledge of the coordination chemistry of Al^{3+} with essential biological ligands. To this end, we report the tertiary structure of the aluminum complex with thymulin studied by the combined use of high resolution NMR spectroscopy (NOESY and HOHAHA experiments) and molecular dynamics calculations.

Thymulin is a well-defined nonapeptide hormone ($\langle \text{Glu}^1\text{-Ala}^2\text{-Lys}^3\text{-Ser}^4\text{-Gln}^5\text{-Gly}^6\text{-Gly}^7\text{-Ser}^8\text{-Asn}^9 \rangle$) produced by the thymic epithelial cells originally isolated from serum [26,27]. It induces or enhances the expression of a number of T-cell markers and functions, notably the Thy-1 differentiation antigen [28]. Its biological activity and antigenicity depend on the presence of zinc ions in the molecule [29]. Interestingly, some other metal cations, particularly Al^{3+} , could compete with Zn^{2+} for the binding to thymulin, inducing a modulated biological activity to the peptide [30].

On the basis of our data analysis, we can conclude that Al^{3+} interacts with the free thymulin to give only one kind of complex, one Al^{3+} for two peptide molecules (1:2 complex), in contrast with the case of Zn^{2+} , where two complexes have been described [31]. Here we report the determination of the three-dimensional structure of the Al^{3+} complex of thymulin by molecular dynamics simulations using as constraints the interproton distances derived from the NMR NOESY data.

2. Experimental

2.1. ^1H NMR experiments

^1H NMR HOHAHA experiments were performed at 400 MHz on a Bruker ARX 400 spectrometer while NOESY experiments at 278 or 298 K were run at 500 MHz on a Bruker AMX 500 spectrometer. NOESY spectra were acquired with three mixing times of 100, 350, and 500 ms. All the NMR data were processed on a 4D-35 TG+ Silicon Graphics workstation using the FELIX software (Biosym, Hare Research).

The measurements were performed with 8 mM solutions of the Al^{3+} -thymulin complex in DMSO-d_6 and in the cryoprotective mixture (80% DMSO-d_6 , 20% H_2O). The water resonance was suppressed by presaturation during the relaxation delay. The interproton distances were derived from the integrated intensities of the off-diagonal NOEs.

2.2. Molecular modeling

The distance geometry calculations were done by using the Biosym DG II program to calculate the initial three-dimensional structures satisfying the experimentally derived upper limit distance constraints. We divided the intensities of the experimental NOE cross-peaks into three separate classes according to the distance restraints d_{ij} : strong for $1.8 \text{ \AA} < d_{ij} < 2.8 \text{ \AA}$; medium for $2.4 \text{ \AA} < d_{ij} < 3.2 \text{ \AA}$ and weak for $3.0 \text{ \AA} < d_{ij} < 4.6 \text{ \AA}$. The 1:2 Al^{3+} -thymulin complex was constructed using bond distances

and angles taken from the standard metal ligand templates of the Biosym force field i.e. $109^{\circ}5$ for the O–Al–O angle and 2.01 Å for the Al–O bond distance: 100 structures were generated by random sampling of the molecular conformations that are consistent with a set of 52 NOE input distance constraints. Two distinct families of structures were obtained that correspond to the two theoretical isomers to be formed in solution when two peptide molecules coordinate to the tetrahedral Al^{3+} cation with different orientations of the peptide ligands. Molecular dynamics (MD) simulations using the Biosym DISCOVER program were performed on the lowest energy structure of each isomer as followed: (a) the initial stage consisted of five periods of 2 ps MD runs at different temperatures (20, 100, 150, 200 and 300 K); (b) a 25 ps MD equilibration period at 300 K with a strong coupling to a thermal bath; (c) a 150 ps final MD run at 300 K. A structure saved every 0.25 ps during the last 30 ps MD run was used for conformational averaging: 150 steps of restrained energy minimization (EM) followed by 350 steps of EM without any distance constraint were applied for the averaged MD conformers. The dielectric constant was chosen equal to $3 \cdot r$ and the non-bonded interactions were evaluated within a 12 Å cutoff.

3. Results and discussion

3.1. Choice of solvent

As outlined above, in aqueous solution the structure determination of Al^{3+} complexes with peptides and proteins is hampered by several difficulties. Consequently, for conformational analysis investigations of these biological systems, the choice of media remains highly problematical. Indeed the microenvironment in which the biological interaction takes place can play an important role in the conformational equilibrium. In order to evaluate the influence of the environment, experiments have been carried out using two different media: (i) an unphysiological solvent, namely DMSO- d_6 , which may simulate roughly the medium at the surface of the cell membrane, where receptors might be located [32], (ii) a cryoprotective mixture of water in an organic solvent, such as DMSO (80% DMSO- d_6 + 20% H_2O), that exhibits, at low temperature, properties close to those of water at room temperature [33].

It is well known that NOESY spectra of small- and medium-sized peptides, in aqueous solution, are characterized by the presence of a very few NOE cross-peaks, as observed with thymulin complexes [34]. These peaks are often of little diagnostic value in conformational studies. However, using a solvent with a higher viscosity such as DMSO (DMSO has a viscosity of 2 centipoise (cp) and 0.8 cp for water at room temperature [35]), a larger number of Overhauser data would appear. Effectively, spectra in DMSO are richer in NOE cross-peaks than the corresponding spectra in water. Furthermore, in DMSO, Al^{3+} is expected to form a more stable complex with thymulin than in aqueous solution. Interestingly, in the 80% + 20% DMSO + water mixture the viscosity increases greatly. Indeed, at 278 K, the DMSO + water cryosolvent is characterized by a viscosity of about 8 cp [35]. Under

those conditions (low temperature and high viscosity), the large amount of NOE data will help us to determine more accurately the three-dimensional structure of the Al^{3+} -thymulin complex in this biomimetic medium [33].

3.2. One-dimensional ^1H NMR studies

One-dimensional ^1H NMR studies were performed in order to determine the influence of Al^{3+} , medium and temperature on the ^1H NMR spectral properties.

In Fig. 1 are shown 1D NMR spectra, corresponding to the thymulin amide region in the presence of Al^{3+} ion, in DMSO-d_6 at room temperature as well as the spectrum in the cryosolvent at 278 K. Comparison with the apo-thymulin (not shown) indicates that the addition of an aluminum salt to a thymulin solution produces important changes in the ^1H NMR spectrum because of the formation of the aluminum complex. These modifications are essentially confined to the downfield region and appear to reflect the changes in the frequencies at which the amide protons resonate. Usually the chemical shift perturbations induced by a diamagnetic metal ion may reflect the direct effect of electron density modifications and/or may result indirectly from a modified conformation of the peptide backbone with, as a consequence, an important dispersion of the NMR signals, in particular the NH signals. Recent results from studies in our laboratory, on the retroviral-type zinc-finger domain of the HIV-2 nucleocapsid protein [36,37], provide evidence that the chemical shift dispersion of signals within the ^1H NMR spectrum clearly demonstrates the presence of a well defined folded compact structure. Surprisingly, the Al^{3+} complexation produces no chemical shift dispersion of the NH signals but rather a marked tendency for these resonances to get closer together. A similar behavior has been observed with Zn^{2+} complexes of thymulin [31] and HIV-1 Tat protein [38]. Nevertheless, if in DMSO-

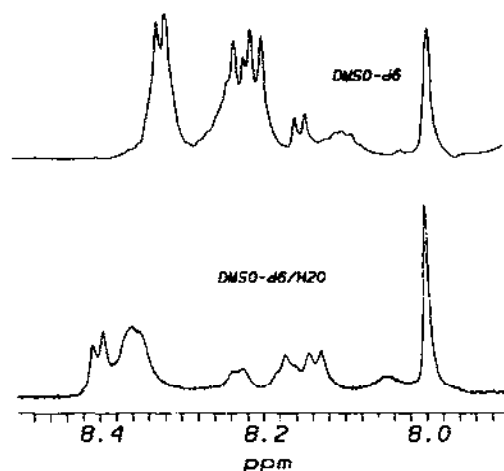


Fig. 1. One-dimensional ^1H NMR spectra of the amide region at 500 MHz of the aluminum complex in DMSO-d_6 at room temperature (top) and, in 80% + 20% $\text{DMSO-d}_6 + \text{H}_2\text{O}$ mixture at 278 K (bottom).

d_6 at room temperature some of the NH resonances degenerate, particularly the A(2)/G(6), Q(5)/G(7) and K(3)/S(8) pairs, on cooling at 278 K ambiguities arising from the observed chemical shift degeneracy are resolved (Fig. 1). Furthermore at this temperature a better dispersion of the NH chemical shifts is observed which is characteristic of stable folded domains in the molecule.

The titration results of the Al^{3+} -bound thymulin complex show that two equivalents of peptide bind one metal ion to form an Al^{3+} -(thymulin)₂ complex [25]. In contrast to the case of Zn^{2+} -thymulin complexation, which involves the formation in situ of two complexes [31], the variations of the NMR amide protons signals, when Al^{3+} is present, are quite interpretable with the presence of only one complex with an association constant $K_2 = 3.0 \pm 0.5 \times 10^6 \text{ M}^{-2}$ [25]. This value is close to that observed with the 1:2 Zn^{2+} complex ($K_2 = 5.1 \pm 0.1 \times 10^6 \text{ M}^{-2}$) [31]. As shown in Fig. 2, thymulin binds the Al^{3+} cation to an extent greater than 87% for an Al^{3+} :peptide ratio (R) of 0.5 while the cation is almost fully bound at a ratio $R = 1$.

3.3. Two-dimensional ^1H NMR studies

Sequence-specific resonance assignments were achieved by following the conventional method proposed by Wüthrich [39] using NOESY and HOHAHA spectra measured consecutively under the same conditions.

The first step was the identification of spin systems corresponding to the different amino acids in the peptide sequence, using the HOHAHA spectrum. An example of an HOHAHA spectrum is shown in Fig. 3. From this spectrum, recorded at room temperature, the degeneracy observed for the amide protons of the A(2)/G(6),

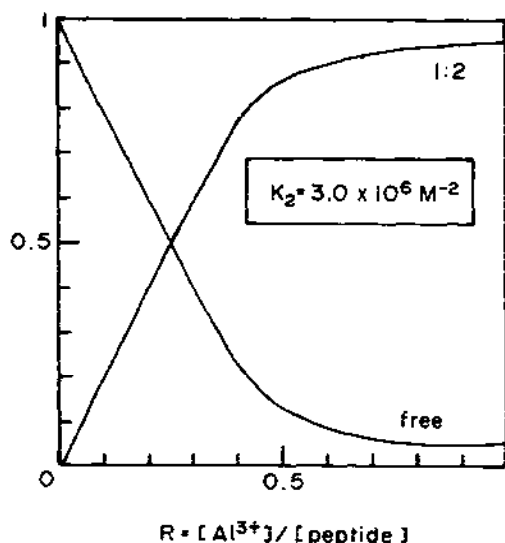


Fig. 2. Calculated variations as a function of the Al^{3+} : peptide ratio (R) of the concentration of free and 1:2 complexed thymulin for a peptide concentration of 0.01 M.

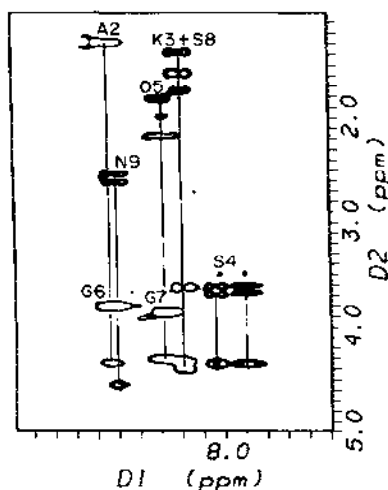


Fig. 3. Fingerprint region of the 400 MHz HOHAHA spectrum obtained for Al^{3+} -thymulin in DMSO-d_6 at 298 K. Direct and relayed through-bond connectivities involving the NH protons and the aliphatic protons are shown with the corresponding labels. Asterisks (*) denote the two S(4)NH signals. Abbreviations follow the standard one-letter code.

Q(5)/G(7) and K(3)/S(8) pairs could be removed at 5 °C. Interestingly, two sets of NMR lines are observed for the S(4)NH resonance at 7.96 and 8.03 ppm respectively. The presence of these two S(4)NH signals provided evidence that, at room temperature, Al^{3+} complexation induces some local changes between the two peptide molecules. In any case, the conformation between these two entities does not seem to be basically different.

The second step was the sequential assignment of the identified spin systems to the corresponding amino acids in the peptide structure. This was mainly based on the $\text{C}\alpha\text{H}(i)/\text{NH}(i+1)$, $\text{NH}(i)/\text{NH}(i+1)$, and $\text{C}\beta\text{H}(i)/\text{NH}(i+1)$ NOE sequential connectivities. The fingerprint region of the NOESY spectra containing connectivities between amide and aliphatic protons is shown in Fig. 4. Clearly, this figure shows that the spectrum in the cryosolvent is richer in NOE cross-peaks than the corresponding spectrum in DMSO. Thus, the $\text{C}\alpha\text{H}(i)/\text{NH}(i+1)$ NOE sequential connectivities and the intra-residue $\text{C}\alpha\text{H}(i)/\text{NH}(i)$ through-bond correlation connectivities, taken together, create three different continuous patterns of sequential connectivities: $<\text{E}(1)$ to A(2), A(2) to S(4), and S(4) to N(9). This region also gives a lot of $\text{C}\beta\text{H}(i)/\text{NH}(i+1)$ connectivities concerning residues $<\text{E}(1)$ to G(6) and S(8) to N(9). In the region of the NOESY spectrum containing cross-peaks between amide resonances (not shown), a stretch of $\text{NH}(i)/\text{NH}(i+1)$ connectivities is identified from residues $<\text{E}(1)$ to A(2). A second stretch is observed from residues G(6) to G(7) and a third one from residues S(8) to N(9). It is to be noted that in DMSO-d_6 at room temperature no cross-peaks are observed in this region. Interestingly the NOEs between nonadjacent residues or long-range NOE effects are very informative. For example, the following NOE connectivities are observed between A(2) β /S(4)NH,

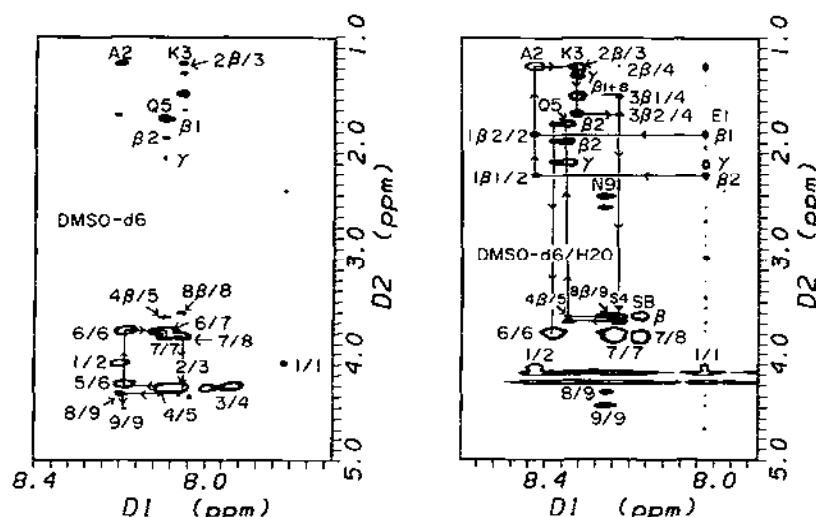


Fig. 4. 500 MHz NOESY spectra for aluminum complex recorded with a mixing time of 350 ms, showing Overhauser effect connectivities from signals of amide protons to C α H and side-chain protons. The left spectrum was recorded in DMSO- d_6 at 298 K, while the right spectrum was recorded in 80% + 20% DMSO- d_6 + H $_2$ O mixture at 278 K.

K(3)NH $_3^+$ /S(4)OH and K(3)NH $_3^+$ /S(8)OH. Finally, a total of 52 experimental restraints based on direct NOE cross-peaks are observed. Among these NOE connectivities 22 are sequential ($i, i+1$ and $i, i+2$), 22 are intraresidual and 8 are backbone–backbone interproton distances. A summary of all sequential connectivities is shown in schematic form in Fig. 5.

3.4. Secondary structure

Earlier ^{27}Al NMR studies on the Al $^{3+}$ –thymulin complex have shown that ^{27}Al resonances were undetectable due to an important broadening [25]. Only an excess of aluminum over the stoichiometry of our complex may be detected by the ^{27}Al

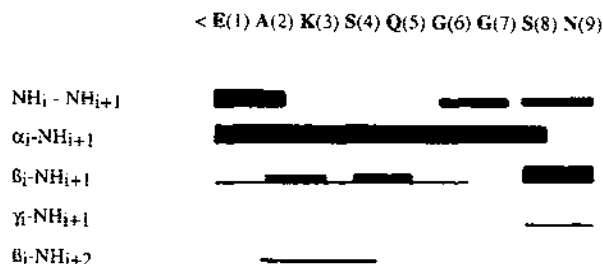


Fig. 5. Summary of sequential (i to $i+1$) NH–NH, C α H–NH, C β H–NH, C γ H–NH and (i to $i+2$) C β H–NH connectivities observed in 2D NOESY spectra of Al $^{3+}$ –thymulin. The thickness of the bars reflects the relative intensities of the cross-peaks observed.

NMR spectroscopy. In the present case no ^{27}Al peaks are observed with an Al^{3+} :thymulin ratio up to 0.5. Beyond this ratio, the progressive addition of aluminum salt is accompanied by an increase in the intensity of the Al resonance due to the excess of Al^{3+} . These results confirm the presence of a 1:2 complex [25]. In fact, the high natural abundance (100%) and sensitivity (20% relative to protons) make the ^{27}Al nucleus favorable for NMR studies. However, its spin number (5/2) results in a nuclear quadrupolar moment so that it is highly sensitive to the symmetry of its local environment and only the Al^{3+} resonances in a perfect cubic symmetry are sharp enough to be detected. Any deviation from pure cubic symmetry brings a characteristic line broadening [40,41]. An Al^{3+} -containing molecule can accommodate either the tetrahedral or octahedral symmetry around the Al^{3+} cation when the ligand size is rather small, as found in $\text{Al}(\text{H}_2\text{O})_6^{3+}$. The tetrahedral disposition remains the only possible form in the presence of a bulky ligand. In view of the size of the thymulin nonapeptide, we think that the two thymulin molecules are ligated rather in a distorted tetrahedral disposition around the Al^{3+} cation than in an octahedral form.

It has been shown previously that the Asn^9 carboxylate C-terminal function and the Ser^4OH hydroxyl group are candidates for complexing the Al^{3+} cation [25]. From a titration study, it appears that one Al^{3+} cation is ligated to two thymulin molecules. These two facts taken together indicate that complexation definitively induces a characteristic compact structure. This secondary structure can be deduced from a qualitative interpretation of the short-range NOEs together with longer-range NOEs between non-adjacent residues. For example, moderate to strong $\text{NH}(i)/\text{NH}(i+1)$ sequential connectivities are observed for residues $< \text{E}(1)/\text{A}(2)$, $\text{G}(6)/\text{G}(7)$, and $\text{S}(8)/\text{N}(9)$ which are characteristic of tight turns.

3.5. Tertiary structure

In the first refinement step, the distance geometry calculations were employed for randomly computing 100 molecular conformations of the 1:2 Al^{3+} -thymulin complex that are consistent with a set of 52 interproton distance constraints derived from the NOESY spectrum. Two distinct families of conformers were obtained in which the two chelating peptide ligands coordinate to a tetrahedral Al^{3+} cation with different orientation. For 60 of them, the two peptide ligands are in the antiparallel disposition while the rest of the conformers are in the parallel disposition.

Nineteen structures of the antiparallel family and 14 parallel structures best satisfying the constraints, for which the root mean square deviations (RMS) between the main chain heavy atoms is less than 3 Å, were selected, averaged within each family and energy minimized. The two resulting conformations were employed as starting coordinates for the restrained 185 ps MD simulations. Analysis of the last 30 ps MD runs shows that the conformations of the two peptide ligands involved in each Al^{3+} -thymulin isomer are practically similar. Fig. 6 depicts the minimized structures of the two conformers. No β -turn was observed in the structure of these peptide ligands around the Al^{3+} cation despite the folding of their C-terminal part. Nevertheless two γ -turns were found for the antiparallel isomer and concerned the

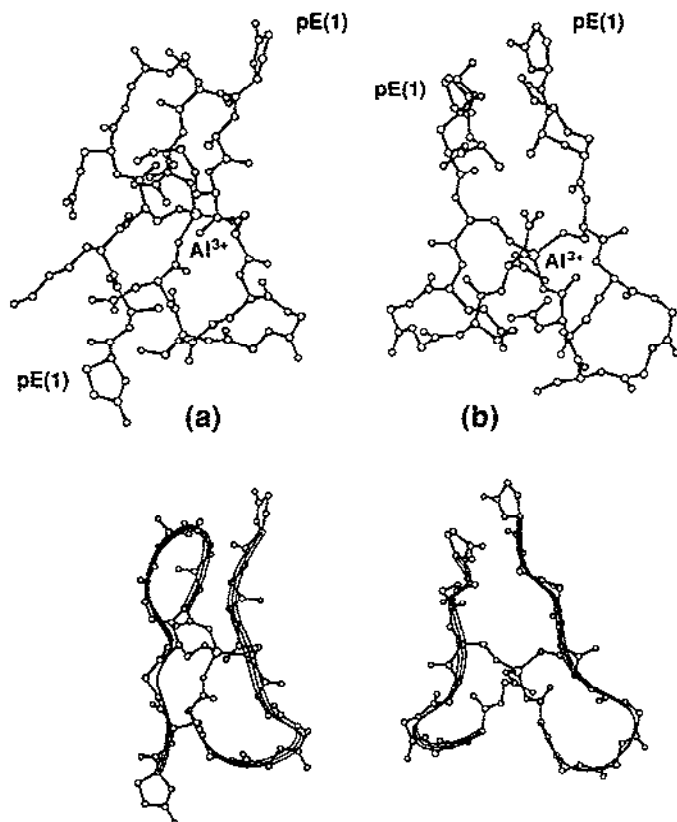


Fig. 6. Minimized structures of the antiparallel (a) and parallel (b) conformers of the Al^{3+} -thymulin complex. The peptide backbones with only heavy atoms are schematically drawn below.

S(4)NH to A(2)CO interaction which closes a 7-membered cycle around the K(3) residue (75% occurrence) and the G(7)NH to Q(5)CO interaction (25% occurrence). These two γ -turns were also present in the parallel disposition with 50% and 60% occurrences respectively. A third γ -turn around the A(2) residue was also found (40% occurrence) for the parallel isomer. For the antiparallel form, the folding of the C-terminal part of the peptide led to the formation of the Q(5)NH to N(9)CO long-range intramolecular interaction (80% occurrence) that was absent in the parallel form. Instead of this, three intermolecular interactions were observed and concerned the Q(5)NH $^{\epsilon}$ to S(8)O $^{\gamma}$ (30% occurrence), the Q(5)NH to N(9)O $^{\gamma}$ (30% occurrence) and the K(3)NH $^{\epsilon}$ to pE(1)O $^{\delta}$ (50% occurrence) interactions. The proximity of the two peptide ligands in the antiparallel form brought closer the K(3)NH of one ligand to the S(4)CO of the other ligand.

The time-averaged structures of the last 30 ps MD runs were minimized. The calculated total energy for the antiparallel form was 104.3 kcal mol $^{-1}$, while that for the parallel form is 121.9 kcal mol $^{-1}$. The difference of 17 kcal mol $^{-1}$ is the result of the gain of 11 kcal mol $^{-1}$ from the bond angle energy term of residues close

to the complexation site, mainly the N(9) residue, in favor of the antiparallel disposition. In addition, the supplement of 6 kcal mol⁻¹ in the total energy of the parallel form is due to the strong intermolecular electrostatic interactions between the two ammonium groups, positively charged, of the lysine residues which are 5.5 Å apart.

The unfavorable growth in the bonded energy of the residues close to the complexation site in the case of the parallel isomer can be explained by the hinder proximity induced by the intermolecular interaction between the Q(5)NH⁺ of one ligand and the S(8)O⁻ of the other ligand. This interaction, which was missing in the antiparallel form, perturbs the geometry of the complexation site around the Al³⁺ cation. It causes larger fluctuations of the O–Al³⁺–O angle values than in the antiparallel form.

4. Conclusion

A 9-residue synthetic peptide corresponding to the amino acid sequence of thymulin, a hormone of thymic origin isolated from serum, has been characterized with regard to its metal binding and structural properties. These experiments have been carried out using two different solvents at two different temperatures: an unphysiological solvent, namely DMSO, which might mimic a lipophilic environment and a cryosolvent (water + DMSO mixture) which has properties close to those of an aqueous environment.

The addition of the Al³⁺ ions to a solution of thymulin results in obvious modifications of the ¹H NMR data. These variations are compatible with the existence of one type of complex with a 1:2 stoichiometry, associating two peptide molecules and one Al³⁺ ion, with an association constant $K_2 = 3.0 \times 10^6 \text{ M}^{-2}$. In this complex, the Asn⁹COO⁻ and Ser⁴OH sites are coordinated to the Al³⁺ ion.

Qualitative analysis of the NOESY spectra strongly supports the hypothesis that, in the two different media, the aluminum complex adopts a similar structure. This structure shows the presence of a folded domain stabilized by a tetrahedral environment around aluminum.

We note that this structure is the first three-dimensional structure of an aluminum-peptide complex determined in solution.

Finally, this study has contributed to a better understanding of the molecular basis for aluminum-containing peptides. Development of similar studies should provide a major advance in our knowledge of the molecular mechanism(s) of aluminum neurotoxicity. Moreover, these data could have counterparts for other biologically active peptides that have not yet been studied with regard to dependence on a metal.

Acknowledgements

This research was supported by the Centre National de la Recherche Scientifique. We thank Dr. P. Lefrancier (Institut Choay-Sanofi, Paris, France) for the gift of

thymulin. Access to the Bruker ARX-400 NMR facilities of the University of Nancy I was deeply appreciated.

References

- [1] H. Sigel and A. Sigel (eds.), *Metal Ions in Biological Systems*, Vol. 24: Aluminum and its Role in Biology, Marcel Dekker, New York, 1988.
- [2] M. Nicolini, P.F. Zatta and B. Corain (Eds.), *Aluminum in Chemistry Biology Medicine*, Cortina International, Verona/Raven Press, New York, 1991.
- [3] B. Corain, A. Tapparo, A.A. Sheikh-Osman, G.G. Bombi, P. Zatta and M. Favaro, *Coord. Chem. Rev.*, 112 (1992) 19–32.
- [4] B. Corain, M. Nicolini and P. Zatta, *Coord. Chem. Rev.*, 112 (1992) 33–45.
- [5] R.B. Martin, *Acc. Chem. Res.*, 27 (1994) 204–210.
- [6] A.C. Alfrey, *Annu. Rev. Med.*, 79 (1978) 93–98.
- [7] M.R. Wills and J. Savory, *Lancet*, ii (1983) 29–34.
- [8] D.R. Crapper, S.S. Krishnan and S. Quittkat, *Brain*, 99 (1976) 67–80.
- [9] P.F. Good, D.P. Perl, L.M. Bierer and J. Schmeidler, *Ann. Neurol.*, 31 (1992) 286–292.
- [10] H. Meiri, E. Banin, M. Roll and A. Rousseau, *Prog. Neurobiol.*, 40 (1993) 89–121.
- [11] F.C. Womack and S.P. Colowick, *Proc. Natl. Acad. Sci. USA*, 76 (1979) 5080–5084.
- [12] J.C.K. Lai, J.F. Guest, T.K.L. Leung, L. Lim and A.N. Davison, *Biochem. Pharmacol.*, 29 (1980) 141–146.
- [13] J.L. Bock and D.E. Ash, *J. Inorg. Biochem.*, 13 (1980) 105–110.
- [14] J.P. Laussac and G. Commenges, *Nouv. J. Chim.*, 7 (1983) 579–585.
- [15] S.J. Karlik, G.A. Elgavish and G.L. Eichhorn, *J. Am. Chem. Soc.*, 105 (1983) 602–609.
- [16] I. Dellavia, J. Blixt, C. Dupressoir and C. Detellier, *Inorg. Chem.*, 33 (1994) 2823–2829.
- [17] D. Dyrssen, C. Haraldsson, E. Nyberg and M. Wedborg, *J. Inorg. Biochem.*, 29 (1987) 67–75.
- [18] S.J. Karlik, G.L. Eichhorn, P.N. Lewis and D.R. Crapper, *Biochemistry*, 19 (1980) 5991–5998.
- [19] De Boni and D.R. Crapper McLachlan, *Life Sci.*, 27 (1980) 1–8.
- [20] G.A. Trapp, *Life Sci.*, 33 (1983) 311–316.
- [21] N. Sigel and A. Haug, *Biochim. Biophys. Acta*, 744 (1983) 36–43.
- [22] Z.M. She, A. Perczel, M. Hollósi, I. Nagypál and G.D. Fasman, *Biochemistry*, 33 (1994) 9627–9636.
- [23] H. Mazarguil, R. Haran and J.P. Laussac, *Biochim. Biophys. Acta*, 717 (1982) 465–472.
- [24] M. Gervais, G. Commenges and J.P. Laussac, *Magn. Reson. Chem.*, 25 (1987) 594–599.
- [25] J.P. Laussac, P. Lefrancier, M. Dardenne, J.F. Bach, M. Marraud and M.T. Cung, *Inorg. Chem.*, 27 (1988) 4094–4099.
- [26] M. Dardenne, J.M. Pléau, N.K. Man and J.F. Bach, *J. Biol. Chem.*, 252 (1977) 8040–8044.
- [27] J.F. Bach, M. Dardenne, J.M. Pléau and J. Rosa, *Nature*, 266 (1977) 55–57.
- [28] J.F. Bach, *Clinics in Immunology and Allergy*, Vol. 3, W.B. Saunders, Philadelphia, USA, 1983, pp. 133–156.
- [29] M. Dardenne, J.M. Pléau, W. Savino, A.S. Prasad and J.F. Bach, *Essential and Toxic Trace Elements in Human Health and Diseases*, Wiley-Liss, 1993, pp. 23–32.
- [30] M. Dardenne, J.M. Pléau, B. Nabarra, P. Lefrancier, M. Derrien, J. Choay and J.F. Bach, *Proc. Natl. Acad. Sci. USA*, 79 (1982) 5370–5373.
- [31] M.T. Cung, M. Marraud, P. Lefrancier, M. Dardenne, J.F. Bach and J.P. Laussac, *J. Biol. Chem.*, 263 (1988) 5574–5580.
- [32] H. Kessler, M. Bernd, H. Kogler, J. Zarbock, O.W. Sorensen, G. Bodenhausen and R.R. Ernst, *J. Am. Chem. Soc.*, 105 (1983) 6944–6952.
- [33] P. Douzou and G.A. Petako, *Adv. Protein Chem.*, 36 (1984) 245–361.
- [34] M.T. Cung and J.P. Laussac, *New J. Chem.* 14 (1990) 293–299.
- [35] P. Amadeo, A. Motta, D. Picone, G. Saviano, T. Tancredi and P.A. Temussi, *J. Magn. Reson.*, 95 (1991) 201–207.

- [36] J.P. Laussac, G. Peyrou, H. Mazarguil, M. Erard, M. Bourdonneau and M.T. Cung, *New J. Chem.*, 17 (1993) 607–612.
- [37] J.P. Laussac, G. Peyrou, M. Bourdonneau, M. Erard, H. Mazarguil and M.T. Cung, *Trends Inorg. Chem.*, 3 (1993) 39–44.
- [38] J.P. Laussac, H. Mazarguil, D. Promé, M. Erard and M.T. Cung, *Metals and Genetics*, Marcel Dekker, New York, 1995, in press.
- [39] K. Wüthrich, *NMR of Proteins and Nucleic Acids*, John Wiley & Sons, New York, 1986.
- [40] J.W. Akitt, *Annu. Rep. NMR Spectrosc.*, 5A (1972) 466–556.
- [41] J.J. Delpuech, in P. Laszlo (Ed.), *NMR of Newly Accessible Nuclei*, Vol. 2, Academic Press, New York, 1983, pp. 153–195.